IET Generation, Transmission & Distribution

Research Article

IET Journals
The Institution of Engineering and Technology

Integration of solar PV into grid using a new UPQC with differential inverter control

ISSN 1751-8687
Received on 30th March 2020
Revised 14th June 2020
Accepted on 22nd June 2020
E-First on 9th July 2020
doi: 10.1049/iet-gtd.2020.0591
www.ietdl.org

Sivarajan Kakkattil Narayanan[1] ✉, *Nirmal Sivarajan*[1], *Jasmin Erakkath Abdu*[1], *Jayanand Balakrishnan*[1]

[1]*GEC, Thrissur, Kerala, India*

✉ *E-mail: sivarajankn1@gmail.com*

Abstract: Integrated photovoltaic (PV) distribution systems voltage stability is of great significance in supporting all connected equipment smooth functioning in the distribution network. Voltage profile maintenance is one of the challenging tasks in PV integration. To maintain a constant voltage profile to a sensitive load of 22 kVA is the main idea of this study. A single-phase PV-integrated distribution system is selected for the study. The novelty is that differential inverters are used for dynamic voltage restorer and distribution static synchronous compensator of the unified power quality conditioner (UPQC). Active power decoupling facility is the main advantage using the differential inverter. The research work objective is to synchronise a 10 kW solar PV system to the distribution system using this new UPQC. The research work discusses and derives the most suitable control strategy for the UPQC with battery energy storage system. A 20 kVA UPQC is designed for the PV integration and to increase voltage stability of the distribution system. The frequency, voltage and reactance/resistance ratio of the distribution system is assumed to be constant. A prototype model of differential UPQC is developed. Experimental and simulation results validate the main objective.

Nomenclature

P_{pv}	power output of the PV
V_{oc}	output voltage in volts of PV module
i_s	current in ampere of the grid
i_i	injected current in ampere of the grid-side of VSI
i_l	current in ampere of the load
i_{ref} *	reference current in ampere of the D-STATCOM
v_{ref} *	reference voltage of the DVR
v	PCC voltage in volts
U_{REF}	input to the PWM

1 Introduction

1.1 Back ground and related works

The utility should supply power at the rated voltage and frequency meeting the power quality (PQ) standards. The present-day PQ issues include high reactive power consumption due to low power factor loads, the low harmonic current burden due to non-linear loads such as converters, battery chargers, mercury vapour lamps, computers, welding sets, arc furnace, etc. Moreover, the loads in distribution supply maynot be in a balance due to single-phase loads. photovoltaic (PV) system is a renewable energy source and is pollution free. Integration of PV will reduce the general energy requirement and losses in the distribution system. Although there are studies that explore the possibility of PVs providing reactive power [1, 2], the most common equipment on the market is deficient in its ability to supply reactive power to the system. Measures to mitigate these PQ issues is the need of the hour in the power sector. Unified PQ conditioner (UPQC) is a compensating device widely used for PQ improvement of the system. It has two Voltage Source Inverter(VSIs), namely distribution static synchronous compensator (D-STATCOM) and dynamic voltage restorer (DVR). Dynamic compensation of reactive power is essential in the system and D-STATCOM is an excellent choice for the above compensation, as it will work with extra active filtering functionality. The DVR is mainly used to eliminate voltage-sag and swell, the two VSIs connected in differential mode (DM) and the differential inverter is explained in one of the sections separately. This paper presents the integration of solar PV to the grid using UPQC.

The PQ indicates voltage quality and frequency stability. The frequency of the Indian grid is stable but the voltage profile requires improvement in certain areas. If the voltage changes by 1%, the power will vary by 2% for impedance type loads. Similarly, if the demand/generation changes by 5%, the frequency changes by 1 Hz for the integrated national (India) Grid. The output power of lights and induction motor will be affected with frequency deficiency.

IEEE standard 1159(1995) governs the PQ of low tension (LT) voltage and currents of the power supply. The allowable dip limits are from 10 to 90%, which last for 0.01 to 0.06 s. The classifications in dip are temporary, instantaneous and momentary. When earth fault occurs in one of the lines, there will be a rise in voltage (swell) in other phases [3]. It is possible to realise active power compensation with the energy storage device at the input of the inverter [4, 5].

The conventional methods of reactive power compensation are using fixed capacitors or reactors, controlled capacitors or reactors, static volt-ampere reactive (VAR) compensators, tap-changing transformers, excitation control of generators etc. These methods suffer from the dynamic adjustment of reactive power. The shunt reactors are in use for reducing line over-voltage and shunt connected capacitors are connected to improve voltage when the system load is high. Shunt capacitors and reactors are not useful in maintaining voltage under dynamic load variations and will not support or provide real power requirement. Usually, D-STATCOM injects reactive power to the grid with proper scheduling of load compensation. Also, active power can be injected into the line if the DC link of D-STATCOM makes use of battery energy storage system (BESS).

To maintain the voltage at any node or bus in a power system, balancing of the reactive power generation and demand at that node or bus is essential. If any mismatch occurs, there will be a change in voltage. Unlike frequency, the voltage is a local parameter to be analysed. Each node or bus plays a role in balancing reactive power. Moreover, the voltage in a bus is inversely proportional to the fault level of that bus. The voltage profile of a power system depends on the V–Q sensitivity. It should be positive in all buses and nodes to maintain voltage stability. If it

is found negative in any one node or bus, then the system enters in voltage instability mode [6]. The issue of voltage sag and swells would be taken care of by DVR with good design and control strategy.

Analysis of the literature review that follows in a separate section shows that the design parameters of LCL filter, BESS, DVR, D-STATCOM and UPQC are missing in most of the proposals. Conventionally, grid-tied inverters for PV integration is in place. In this research work, the author aims to mitigate the gap by developing a new UPQC using differential inverters for both DVR and D-STATCOM for PV integration with the design of all the necessary parameters.

1.2 Major contributions

i. The novelty is that a single-phase UPQC, rated at 20 kVA, using differential inverters, is proposed with BESS for the PV Integration. The active power decoupling functionality of differential inverter ensures ripple-free voltage and current in the dc input (battery) of D-STATCOM. It also injects the active power of the PV source, the entire reactive power of load and reactive losses of the system. The DVR, connected in DM, takes care of sag and swell in the system.
ii. The design is economical considering low DC link voltage, low capacity for BESS, the low voltage level for PV System and low rating of inverter switches. The author's design ensures good tracking by the D-STATCOM.
iii. A prototype model of the UPQC using a differential inverter is developed in the research laboratory with D-space controller, simulation studies are carried out for linear, non-linear and transient loads in grid and PV sides and the results are validated.

1.3 Organisation of the paper

This paper is organised into the following sections. Section 1 deals with Nomenclature and the introduction. Section 2 deals with the review on PV-integrated distribution system and UPQC. Section 3 deals with the differential inverter. Section 4 deals with circuit topology of UPQC. Section 5 describes the mathematical derivation of reference/injected currents. Section 6 describes the case study of 20 kVA UPQC in the PV-integrated distribution system. Discussion on results is presented in Section 7. Section 8 deals with the conclusion.

2 PV-integrated distribution system and UPQC

The UPQC is one of the custom power devices which consists of D-STATCOM and DVR. D-STATCOM is in shunt connection with the distribution line. The primary function lies in injecting or absorbing the reactive power set by the controller. It is possible to achieve unity power factor in source current if the D-STATCOM pumps entire reactive power and losses. Using the best control algorithms, we obtain proper tracking (injected current is the same as that of the reference current) and total harmonic distortion (THD) reduction of source current. So the current reference generation is significant in the control strategy. D-STATCOM injects or absorbs active power with the BESS in the DC link.

DVR is connected in series with the line and used for sag and swell mitigation. The load voltage remains constant irrespective of disturbances in current or voltage. UPQC, a combination of D-STATCOM and DVR, is used for PQ improvement of the system.

Patel *et al*. [7] presented a novel control, namely synchronous reference frame theory-based power angle (PAC) for UPQCDG to integrate solar PV system to the grid effectively. Reactive power-sharing of load between series and active power filters with a better kVA utilisation and good PQ is a major advantage. The system was tested using simulation, though experimental validation is not provided. Chaudhari *et al*. [8] reviewed the impacts and challenges caused by PV integration in the distribution network. The research puts forward a number of solutions to various problems of voltage rise existing due to PV penetration. The authors have suggested usage of pumped hydro energy storage systems and other storage systems as a solution to voltage rise mitigation for future work.

Luo *et al*. [9] presented the optimal location and size of DG with solar farm functioning as STATCOM. A sensitivity analysis test procedure has been employed to study the impact of STATCOM in voltage recovery. The proposed optimisation model could have been more practical and the economic profits of the scheme shall be quantified. Sakar *et al*. [10] studied the hosting capacity and harmonic distortion limits of the PV-based DG units using PQ and energy efficiency parameters. Authors used the harmonic penetration ratio to analyse the impact of harmonics on the hosting capacity. Nieto *et al*. [11] investigated the effect of a wind generation on a power grid. Authors emphasise the importance of energy storage systems in regulating the power injected from distributed generation.

Fujitha and Akagi [12] proposed the integration of DVR and DSTATCOM for UPQC. A 20 kVA UPQC was designed to verify its effectiveness and viability of performance. Aredes *et al*. [13] presented a universal power line conditioner. This paper is, however, an extension of the conventional instantaneous real and reactive power theory. Tolbert *et al*. [14] proposed a multilevel diode clamped controller-based universal power conditioner, wherein the authors use multilevel PWM to increase switch utilisation. Ghosh *et al*. [15] presented the simultaneous voltage and current control of UPQC. In the voltage control mode, the voltage of a distribution bus is balanced. Meanwhile, load compensation is also obtained, leading to balanced sinusoidal currents from the distribution system bus in the current control mode. Haghighat *et al*. [16] proposed an instantaneous theory-based control of UPQC for transient and steady-state conditions. The scheme also identifies a method to reduce oscillations in power during transient conditions. Han *et al*. [17] presented a new configuration of UPQC for LT applications. By increasing the number of H-bridge modules, the operation voltage can be expanded.

Kolhatkar and Das [18] experimented on a single-phase UPQC with minimum VA loading. This was achieved when the DVR-injected voltage at the right angle to the grid. Hingorani *et al.* [5] presented types and categories of various controllers with different control strategies. Central Electricity Regulatory Commission and others [19] published the Indian Electricity Grid Code with effect from 1 April 2006. Hingorani *et al*. [5] explained various controls for STATCOM.

Padiyar [4] explained the synchronous reference frame(SRF) and directed current extraction techniques for D-STATCOM installed in three-phase, four-wire system. Bhim Singh and Ram Niwas proposed ADALINE control for PMSG-based DG set to reduce THD. Pawar *et al*. [20] proposed the D-STATCOM for load compensation in the line for voltage stability and power factor improvement using instantaneous reactive power (IRP) control strategy. The performance of the device was analysed for unbalanced and non-linear loads. With the help of this strategy, a balanced source current for unbalanced loading is achieved. Saradva *et al*. [21] proposed D-STATCOM for frequency regulation and voltage regulation of the distribution system. The system is not tested for transient loading. However, both real and reactive power compensation was achieved. The comprehensive study of D-STATCOM configurations has been presented by Singh *et al*. [22]. Bina *et al*. [23] presented the design and installation of 250 kVAR D-STATCOM in one of the distribution substations in Tehran. Singh *et al*. [24] presented different control strategies viz. IRP Theory, SRF theory, SRF theory and ADALINE control for D-STATCOM. The operating characteristics of the D-STATCOM and the demonstration of practical results were carried out successfully by the authors.

3 Differential inverter

The DM buck inverter consists of two dc–dc buck converters, as shown in Fig. 1, with two operating modes, namely the DM and the common mode (CM). DM transfers active power while the CM compensates the second-order ripple power arising from the differential mode. Fig. 2 shows the CM circuit diagram, which is self-explanatory. The design of components of the inverter is

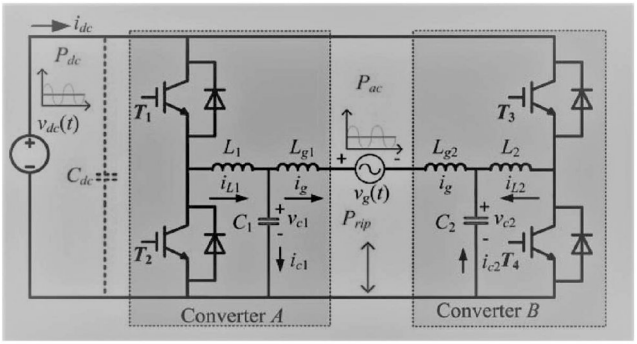

Fig. 1 *Circuit diagram of the differential inverter*

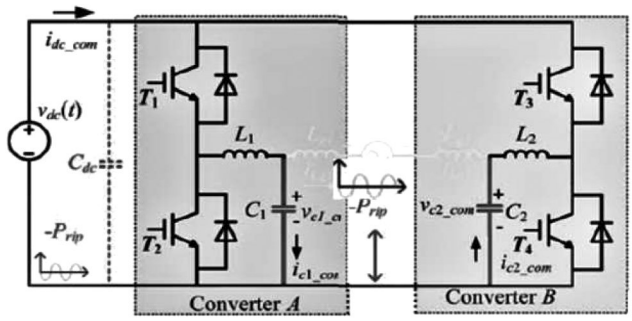

Fig. 2 *CM circuit diagram of the differential inverter*

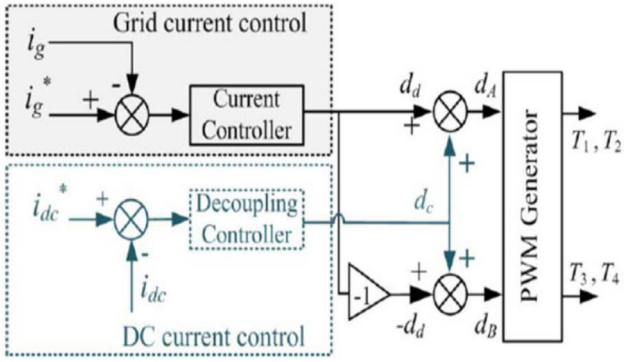

Fig. 3 *Overall control structure of the differential inverter*

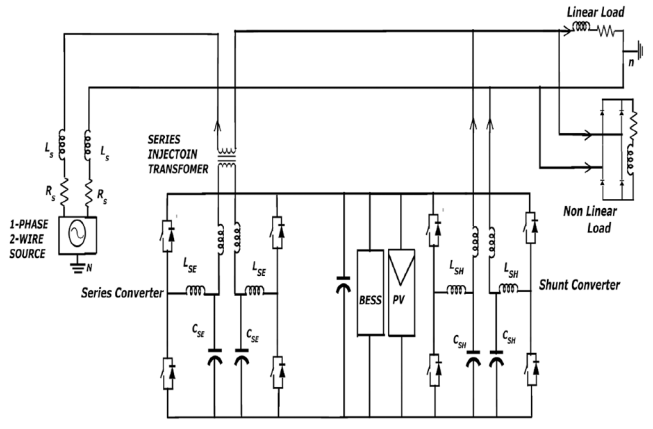

Fig. 4 *Circuit diagram of 1-phase UPQC using differenial inverters*

discussed separately in the following section [25]. The control strategy is also discussed in a separate section.

Fig. 3 shows the control circuit of the differential inverter. This circuit has an additional DC compensation that achieves power decoupling. The battery current will be free from double frequency ripples and the life of the battery will be more if decoupling is employed. Moreover, the value of the ripple capacitor can be reduced.

Table 1 System parameters

Item description	Values for simulation
source voltage	230 V, 50 Hz
feeder impedance	0.2 + j0.2 Ω
linear load	Z = 2.09 + j1.09 Ω
other loads	rectifier
	(RL): 40 + j31.4 Ω
20 kVA	$V_{dc} = 360$ V, $C_{dc} = 7$ mF
UPQC	$L_1 = 2$ mH, $L_2 = 0.4$ mH
	$R_d = 5\,\Omega$
	$C = 36\,\mu F$

4 Circuit topology of UPQC

Fig. 4 shows the circuit diagram of single-phase UPQC using differential inverters. The source is modelled as 230 V, single-phase system, (R-phase of a three-phase, four-wire system and neutral) is considered as the distribution grid. The DC Link voltage is 360 V DC. A BESS of 360 V, is proposed in the DC link [22].

The shunt D-STATCOM controller is mainly intended to inject reactive power to the grid at the PCC. Unity power factor can be achieved if no reactive current is taken from the source. The reference current should be derived by forcing the source to deliver real power and losses only. The DVR is used to mitigate the voltage sag and swells in the network. The system parameters are shown in Table 1.

4.1 Design of compensator components

Robustness of the controller means good tracking and better stability during the transient response. This, in turn, depends on the input DC voltage (V_{dc}), DC link capacitor (C_{dc}) and filter.

(i) *DC bus capacitor*: The capacitor C_{dc}, depends on the instantaneous energy available to the D-STATCOM during transients. According to energy conservation theory

$$\frac{1}{2}C_{dc}(V_{dc}^2 - V_{dc1}^2) = V(aI)t \tag{1}$$

where V_{dc} is the reference dc voltage and V_{dc1} is the minimum voltage of dc bus, 'a' is the over loading factor, V is the voltage, I is the current and t is the time. Considering the dc bus voltage V_{dc1} = 350 V, V_{dc} = 360 V, I = 87 A, t = 1 ms and overload factor of 1.2, C_{dc} is ∼7 mF

(ii) *Design of LCL filter*: In designing LCL filter, we have to consider the cost of inductor, resonance frequency f_{res}, damping resistor R_d and switching frequency attenuation f_{sw}. The following formula is useful in calculating the inductor value

$$L_1 = \frac{V_{dcref}}{4hf_{max}} \tag{2}$$

Consider only L_1 of LCL filter is used. The proposed rating of compensator is 20 kVA, a current ripple of 10% comes to 8.7 A. Taking V_{dc} as 360 V and f_{max} as 10 kHz, L_1 is 2 mH. Once L_1 is chosen, L_2 and C need to be computed to eliminate higher-order harmonics.

Referring to Fig. 5 and neglecting all resistances including R_d, the transfer function of LCL filter combination is arrived as follows:

$$G_F(s) = \frac{I_1(s)}{V_1(s)} = \frac{s^2 + (1/L_2C)}{sL_1(s^2 + (L_1 + (L_2/L_1L_2C)))} \tag{3}$$

where I_1 is the inverter current and V_1 is the inverter voltage

$$\frac{I_{f2}(s)}{V_{inv}(s)} = \frac{1/L_1L_2C}{s(s^2 + (L_1 + (L_2/L_1L_2C)))} \tag{4}$$

$$\frac{I_{f2}(s)}{I_{f1}(s)} = \frac{1/L_2C}{s^2 + (1/L_2C)} \tag{5}$$

$$P = z\sqrt{1+k} \tag{6}$$

where

$$f_{\text{res}} = \frac{1}{2\Pi}\sqrt{\frac{1+k}{kL_1C}} \tag{7}$$

and

$$k = L_2/L_1 \tag{8}$$

Resonance frequency f_{res} is taken as 2400 Hz, which is 20% higher than the highest order of 40 (2000 Hz). Value of k should be less for minimum loss and good efficiency. C is designed as 36 μF. Taking k as 0.172, L_2 = 0.34 mH [26]

5 Control strategy of UPQC

The schematic representation for the control strategy of UPQC is given in Fig. 5 using the circuit topology as per Fig. 4

5.1 Control of D-STATCOM

First of all, it is required to calculate the active power and reactive power of the load using a positive sequence power measurement tool available in the Simulink library. Adding the losses of the inverter to the active power and subtracting the PV power is required. The power so obtained is the power to be delivered by the source. Then, we have to calculate the reference current for this source power using the function block as i_s.

$$i_s = 320\frac{P_s}{v_1^2}\sin(wt) \tag{9}$$

where P_s is fundamental active power of source and v_1 is the positive sequence voltage at the PCC. Then the error between the total load current i_l and i_s is $i_{\text{ref}}*$. We have then compared this current with the injected current i_i of the inverter. This is given to a PR controller and the output is U_{REF}. This is given to a PWM for pulse generation of pulse for leg A of the D-STATCOM. U_{REF} is inverted and is provided as the second PWM generation pulse for leg B of the D-STATCOM. The generated voltage is filtered using the LCL filter, as shown in the circuit diagram. The D-STATCOM injects the active power of the PV source and the entire load reactive power demand (the DM connection takes care). The CM connection is used to circulate the ripple power through switches and capacitors. The filter capacitance generates the second-order frequency component of active power and is connected between the alternating current (AC) terminal and the negative side of the battery.

5.2 Control of DVR

The phase-locked loop (PLL) receives the source voltage as the input and the output is wt. Using a function block the $v_{\text{ref}}*$ is obtained as

$$v_{\text{ref}}^* = 320\sin(wt) \tag{10}$$

and its error with the load voltage, v_l is given to a PR controller. The output is U_{REF} and given to a PWM for pulse generation of leg A of the dc–dc converter of the DVR. U_{REF} is inverted and given to the second PWM for the generation of pulse for leg B of the DVR. The generated voltage is filtered using the LCL filter, as shown in the circuit diagram. This voltage is given to the injection

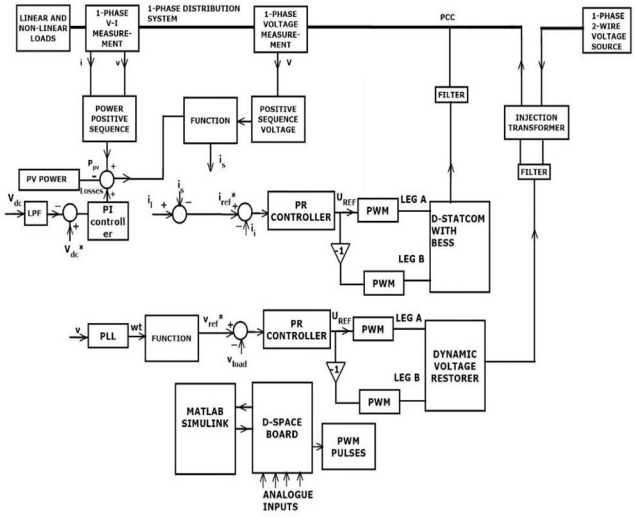

Fig. 5 *Simple block diagram for the control strategy for UPQC*

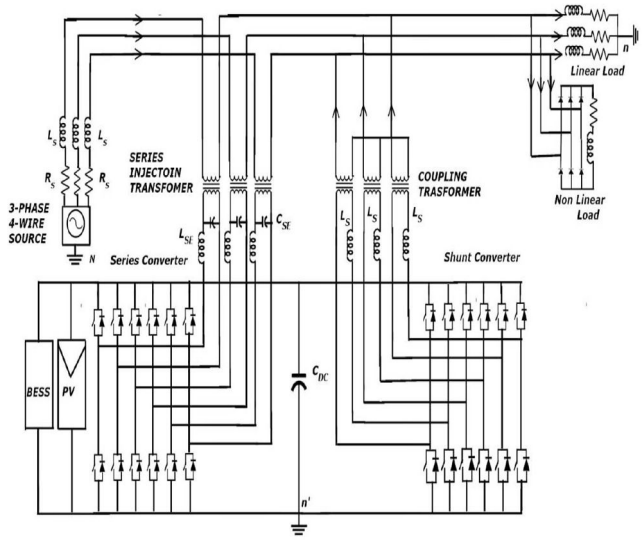

Fig. 6 *Simple circuit diagram of UPQC for three-phase distribution system with PV integration*

transformer primary. The secondary of the injection transformer is in series to the line, as illustrated in Fig. 5. During sag and swell, the DVR injects appropriate voltages to the system and maintains the load voltage. Here the DM is used to transfer the power, whereas the CM is used to bypass the ripple power.

6 Case study of PV-integrated system

The PV-integrated distribution system and the UPQC connection is shown in Fig. 6, which is for a three-phase four-wire system. The connection of D-STATCOM and DVR is in DMs, two legs for each phase. The topology, as shown in Fig. 5, is designed for the system case study. The distribution grid comprises of single-phase, 230 V system (R-phase of a three-phase, four-wire system and neutral). All aluminium conductor (AAC) 7/3.1 conductor is selected for the distribution feeder. The length of the feeder is 1 kM and its R and X values are 0.2 ω kM. The peak load of the distribution feeder is 22 kVA (20 kW and 10 kVAR). The short circuit capacity is about 500 kVA as per the Electrical Transient Analyzer Program (ETAP) 16.2 analysis. The loads, as mentioned in Table 1, are used for simulation. The total active power is 20 kW and reactive power is 10 kVAR. The power factor is around 0.9. When $\Delta V/V$ = 10%, the reactive compensation required is 50 kVAR. Assuming a 2% variation in voltage, a D-STATCOM of 10 kVAR rating, for maintaining the voltage alone, is presently required at the PCC. The design capacity is 15 kVA for PV integration and voltage stability [23]. Assuming a voltage sag/swell of 10% the voltage to

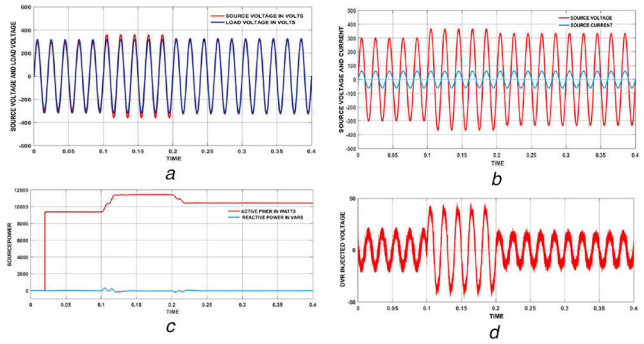

Fig. 7 *Wave forms*
(a) Voltage of source and load, ***(b)*** Source voltage and current, ***(c)*** Source active power and reactive power, ***(d)*** DVR-injected voltage

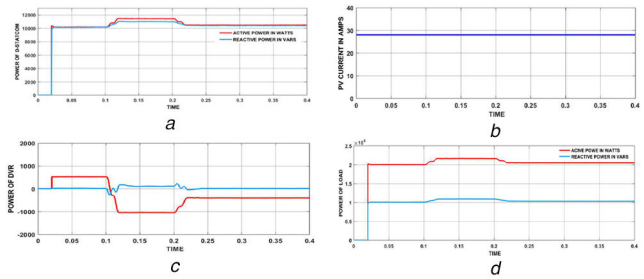

Fig. 8 *Wave forms*
(a) D-STATCOM power, ***(b)*** PV current, ***(c)*** DVR power, ***(d)*** Load power

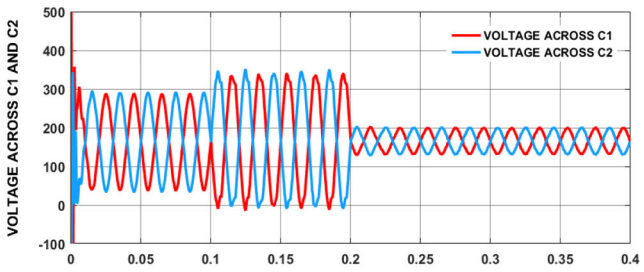

Fig. 9 *Wave forms showing voltage across capacitors C1 and C2 of DVR*

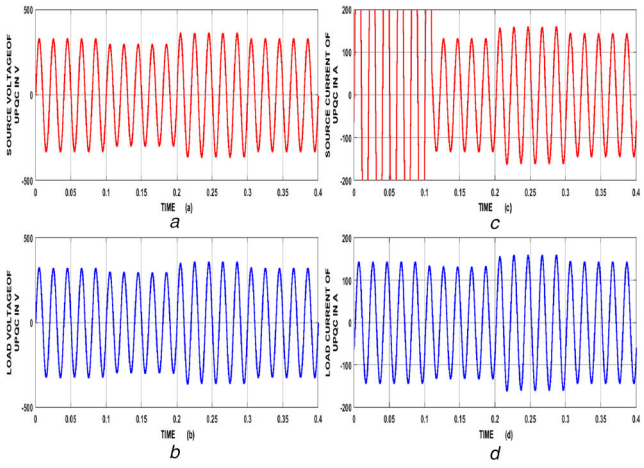

Fig. 10 *Wave forms showing*
(a) Source voltage, ***(b)*** Load voltage, ***(c)*** Source current during transient loading, sag, swell and normal conditions, ***(d)*** Load current without UPQC

be injected by the DVR is 23 V. The current through the injecting transformer is around 50 A including losses. The kVA rating of the injection transformer is 23 * 50 = 1150 VA. This comes to around two kVA for design purpose, which is sufficient for large sag/swell. The UPQC capacity is proposed as 20 kVA

6.1 Design of BESS

The solar-embedded MATLAB function is used for the simulation of the PV system. The open-circuit voltage is 360 V, while the connected load is 10 kW operated for 10 h. Therefore, the total capacity of the battery bank is 100 kWh. Each cell has a rating of 12 V. As the DC BESS voltage is 360 V, it is needed to arrange 30 cells in series. The ampere-hour capacity of each cell is 100 Ah. The total ampere-hour rating is 278 Ah. Hence it is mandatory to have three parallel sets of 30 series cells.

7 Results and discussions

7.1 Simulation results of proposed UPQC

A 20 kVA UPQC has been designed in a PV-integrated distribution system using a reduced DC link voltage of 360 V and simulated in MATLAB R2016a using ode23tb solver. The system parameters as per Table 1 are used for simulation. The main objectives are

i. To maintain a constant voltage of 320 sin(ωt) (root mean square (RMS) value, 226 V) for a sensitive load of 22 kVA (linear and non-linear) irrespective of transient loading, sag and swell in the system.
ii. To maintain uniform and pure sine wave of 60 sin(ωt) for the source current during the entire period of simulation.
iii. Another objective is to maintain unity power factor for the source current.
iv. THD reduction and PQ improvement is another factor are other factors of concern.

The waveform, depicted in Fig. 7*a* represents the source voltage and load voltage. The sag of 10% is initiated at 0 s for a duration of 0.01 s. The swell of 10% is initiated at 0.1 s for 0.01 s that is up to 0.2 s. A programmable voltage source is used for creating sag and swell. The instantaneous load voltage is 320 sin(ωt) and the RMS value is 226 V for the entire period of simulation. Fig. 7*b* shows the source voltage and the source current. The power factor is unity and the peak value of current is about 46 A, which represent the 10 kW power delivered by the source. Fig. 7*c* shows the source power and no reactive power is delivered. Fig. 7*d* shows the injected voltage of DVR. The power of the DVR is depicted in Fig. 8*a*. Fig. 8*b* shows the current in ampere of the PV source, which is 27 A. Fig. 8*c* shows the power of D-STATCOM. The real power is 10 kW and reactive power is 10 kVAR. The power of the load is depicted in Fig. 8*d*. The real power is 20 kW and the reactive power is 10 kVAR. Fig. 9 shows the waveforms of the voltage across the capacitors C1 and C2 of the DVR for the entire simulation period.

Figs. 10 and 11 shows the waveform of source voltage, load voltage, source current and load current during transient loading, sag, swell and normal loading without UPQC and with UPQC, respectively. Fig. 10*a* shows the waveform of source voltage. From time 0 to 0.1 s the peak value is 325 V, from time 0.1 to 0.2 s there is a sag of 23 V and the peak value is 292.5 V, from time 0.2 to 0.3 s, there is a swell of 23 V and the peak value is 357.5 V and from time 0.3 to 0.4 s, normal voltage is applied to the UPQC and the peak value is 325 V. Fig. 10*b* shows the load voltage wave form without UPQC. This figure is similar to Fig. 10*a*. Fig. 10*c* shows the waveform of the source current of the UPQC. From time 0–0.1 s, a transient load of 425 A is applied. From 0.1 to 0.4 s, there is a loading of 22 kVA in the system. The peak currents in the respective periods are 601, 130, 160 and 145 A as per the figure. Fig. 10*d* shows the load current of the UPQC for a connected load of 22 kVA as per the source voltage indicated in Fig. 10*a*. The values are 145, 130, 160 and 145 A.

Fig. 11*a* shows the source voltage with UPQC in service. The values of voltages are similar to that of Fig. 10*a*. Fig. 11*b* shows the load voltage waveform of the UPQC and the peak value is 320 V as seen from the figure. Fig. 11*c* shows the waveform of source current with same transient loading and same loading as per Fig. 10*c*. It is clearly seen that the source current is uniform from time 0.1 to 0.4 s and the peak value is 60 A. (i_s = 60 sin(ωt). This current is the equivalent current for 10 KW active power and losses in the

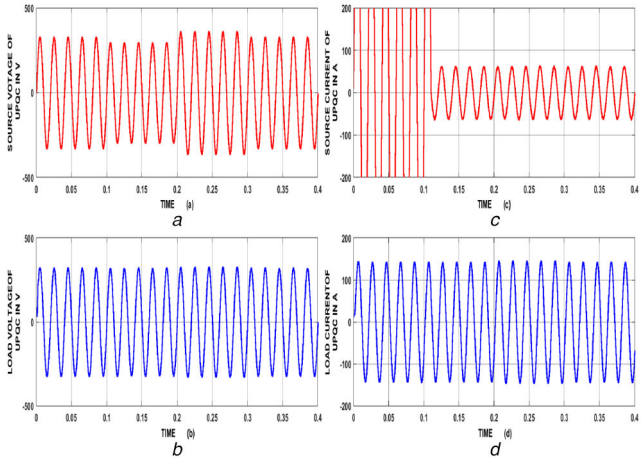

Fig. 11 *Wave forms showing*
(a) Source voltage, ***(b)*** Load voltage, ***(c)*** Source current during transient loading, sag, swell and normal conditions, ***(d)*** Load current with UPQC

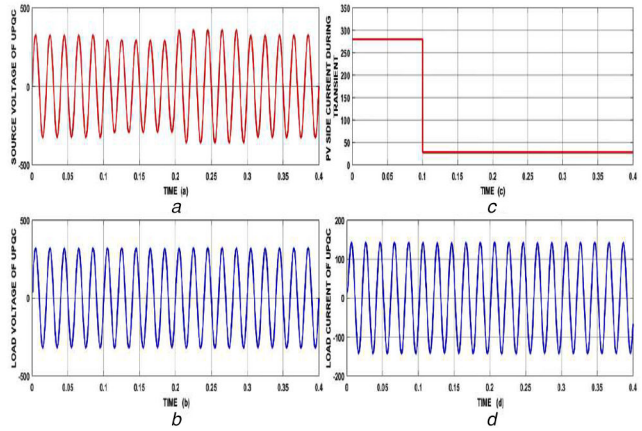

Fig. 12 *Wave forms showing*
(a) Source voltage, ***(b)*** Load voltage, ***(c)*** PV side current during transient, ***(d)*** Load current with UPQC

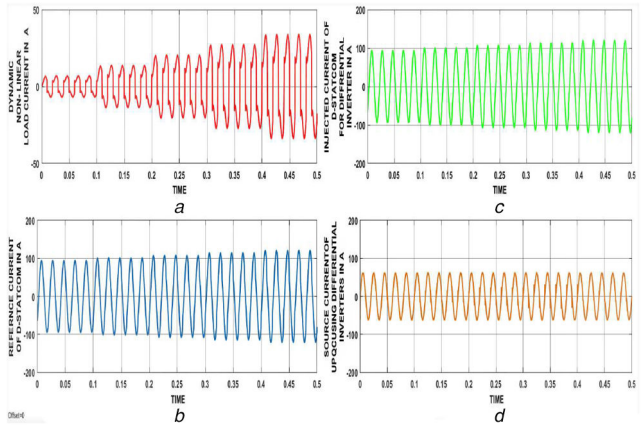

Fig. 13 *Wave forms showing*
(a) Dynamic non-linear loading, ***(b)*** Reference current of D-STATCOM, ***(c)*** Actual-injected current of D-STATCOM using differential inverter, ***(d)*** Source current of UPQC using differential inverters

system. The source current maintains the unity power factor during sag and swell with UPQC in service. Fig. 11*d* shows the waveform for load current for a load voltage of 320 sin(ωt) which is 140 A (peak). Simulation results validated all the objectives mentioned above.

Fig. 12*a* shows the source voltage with UPQC in service with a transient loading in the PV side. The values of voltages are similar to that of Fig. 11*a*. Fig. 12*b* shows the load voltage waveform of the UPQC and the peak value is 320 V as seen from the figure. Fig. 12*c* shows the waveform of PV side current with a transient loading of 280 A DC from time 0 to 0.1 s. This is achieved using switch control and delay timer. The transient load is taken as 10 times that of the normal PV integration of 10 kW (28 A). From time 0.1 to 0.4 s the PV side load is 28 A. Fig. 11*d* shows the waveform for load current for a load voltage of 320 sin(ωt) which is 140 A (peak). During the transient fault on the PV side also, the UPQC was able to maintain the load voltage and load current. Simulation results validated all the objectives mentioned above.

7.2 Comparison of simulation results of conventional UPQC and proposed UPQC

Simulation studies are carried out to compare the performance of conventional H-bridge single-phase UPQC and proposed UPQC. The system parameters as per Table 1 are used for both UPQCs. The main objectives of this simulation are

i. To analyse the tracking of the control system of the D-STATCOM of the proposed UPQC and conventional UPQC. Tracking is the ability of the inverter to inject the exact reference current set by the controller.
ii. To find out a practical system, with lot of harmonics and non-linearity, such as residential loads and PV penetration. The output of PV generation is DC voltage. It is to be converted to AC voltage before connecting to the grid. Therefore, inverters are required for conversion from DC to AC. This will increase harmonics and non-linearity in the line.
iii. To compare conventional UPQC and proposed UPQC, by conducting simulation studies with dynamic change in non-linear load, keeping the linear load constant. Then the reference current and injected current wave forms are analysed.
iv. To conduct FFT analysis of the injected currents in both cases to substantiate the simulation results.
v. To conduct FFT analysis of the source currents in both cases to substantiate the simulation results.
vi. To tabulate the results of FFT analysis.
vii. To find out the advantages and disadvantages of the two UPQCs after analysing the results of simulation and FFT analysis.

Fig. 13*a* shows the waveform for dynamic non-linear loading using proposed UPQC. The loading is done from time 0 to 0.5 s with five spells of 0.1 s each, using breaker control. The load is about 1.1 kW in each spell. The peak value is around 6.6 A in each spell, the highest being 33 A during the last spell. Fig. 13*b* shows the reference current of the D-STATCOM of the UPQC ($i_{\text{ref}} = i_{\text{l}} - i_{\text{s}}$). The peak value of the reference current will change according to the changes in the non-linear load, which is evident from the figure. Fig. 12*c* shows the actual injected current of the D-STATCOM. In this case, it is same as that of Fig. 13*b*, which means that the injected current follows the reference current. Fig. 13*d* shows the waveform of the source current of UPQC using differential inverters which is 60 sin(ωt). The THD of source current is 2.18% for the time period 0.4–0.5 s.

Fig. 14*a* shows the waveform for the dynamic non-linear loading of the UPQC using conventional H-bridge inverters which is similar to Fig. 13*a*. Fig. 14*b* is the reference current of the D-STATCOM of this inverter which is similar to Fig. 13*b*. Fig. 14*c* shows the actual injected current of the conventional H-bridge D-STATCOM, which is distorted. Fig. 14*d* shows the waveform of the source current of the UPQC, using conventional H-bridge inverter, which is also distorted. The THD of the source current is 23.16 % for the time period, 0.4–0.5 s. Comparing the above Figs. 12 and 13, it is evident that good tracking is achieved in the D-STATCOM using differential inverters.

The FFT analysis of the injected currents for both topologies is carried out for the entire period of 0.5 s. Figs. 15 and 16 show the FFT analysis of injected currents for proposed UPQC and conventional UPQC, respectively, for the worst case of non-linearity (time: 0.4–0.5 s). The results for the entire FFT analysis are tabulated in Table 2. Here H1, H2, H3, H5, H7 are the

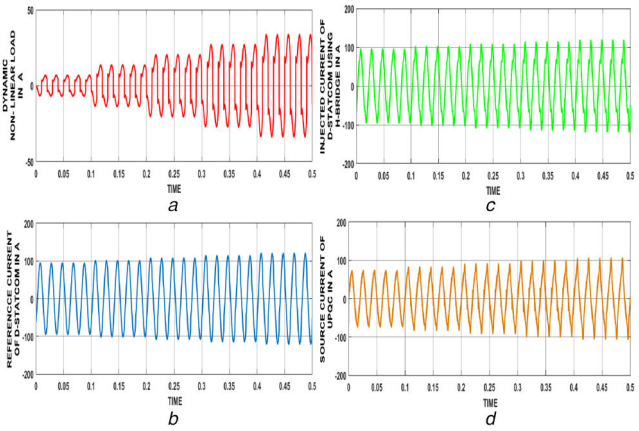

Fig. 14 *Wave forms showing*
(a) Dynamic non-linear loading, ***(b)*** Reference current of D-STATCOM, ***(c)*** Actual injected current of D-STATCOM using conventional H-Bridge inverter, ***(d)*** Source current of UPQC using conventional H-Bridge inverters

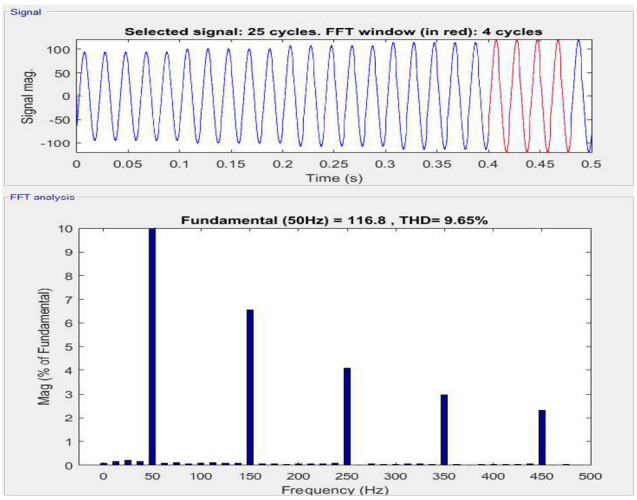

Fig. 15 *Figure showing showing the FFT analysis of injected current of D-STATCOM of proposed UPQC using differential inverter*

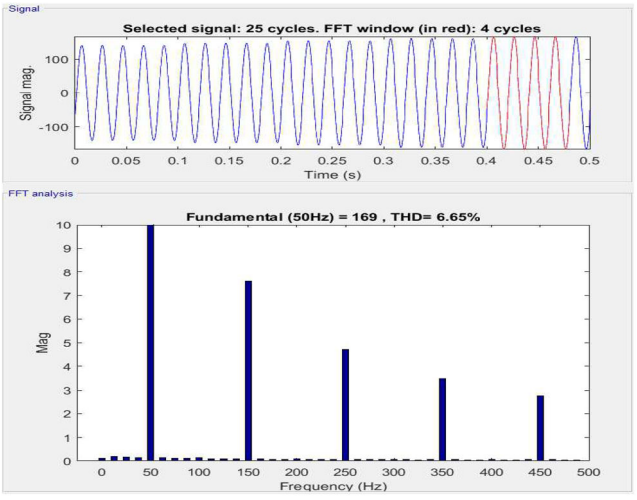

Fig. 16 *Figure showing the FFT analysis of injected current of D-STATCOM using conventional H-Bridge inverter of UPQC*

fundamental component, second-order, third order, fifth-order and seventh order of the injected current, respectively. From Table 2, it is clear that the fundamental component in conventional D-STATCOM deviates largely from the reference current. However, the injected current follows the reference current in the proposed D-STATCOM using the differential inverter. Even harmonics are very less in both topologies. Odd harmonic components are almost the same in both topologies.

Table 2 FFT analysis of injected current

Time period	Reference current peak, A	H-bridge inverter H1, H2, H3, H5, H7 peak, A	Differntial inverter H1, H2, H3, H5, H7 peak, A
0–0.1	93	143, 0.15, 1.31, 0.92, 0.66	92, 0.13, 1.3, 0.95, 0.69
0.1–0.2	99	149, 0.13, 2.88, 1.93, 1.37	98, 0.13, 2.91, 1.88, 1.37
0.2–0.3	105	156, 0.12, 4.44, 2.91, 2.09	105, 0.12,4.45, 2.86, 2.08
0.3–0.4	112	163, 0.13, 6.01, 3.90,2.81	111, 0.12,5.95, 3.83, 2.78
0.4–0.5	120	169, 0.13, 7.65, 4.73, 3.48	117, 0.09, 7.63, 4.73, 3.46

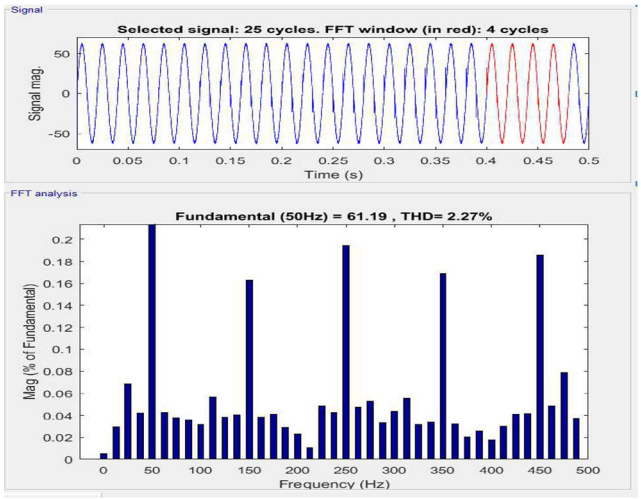

Fig. 17 *Figure showing the FFT analysis of source current of proposed UPQC using differential inverter*

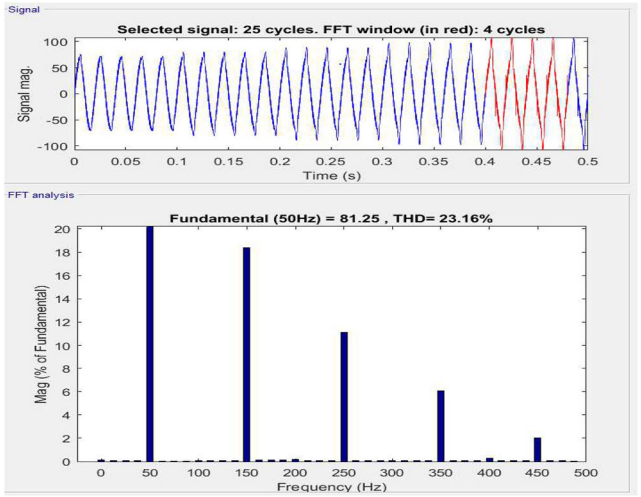

Fig. 18 *Figure showing the FFT analysis of source current of UPQC using conventional H-Bridge inverter*

The FFT analysis of the source currents for both topologies is carried out for the entire period of 0.5 s. Figs. 17 and 18 show the FFT analysis of source currents for proposed UPQC and conventional UPQC, respectively, for the worst case of non-linearity (time: 0.4–0.5 s). The results for the entire FFT analysis are tabulated in Table 3. Here H1, H2, H3, H5, H7 are the fundamental component, second-order, third order, fifth-order and seventh order of the source current, respectively. From Table 3, it is clear that the fundamental component of source current in

Table 3 FFT analysis of source current

Time period	Reference current peak, A	H-bridge inverter H1, H2, H3, H5, H7 peak, A	Differntial inverter H1, H2, H3, H5, H7 peak, A
0–0.1	60	66.8, 0.15, 2.86, 1.56, 1.00	62.2, 0.08, 0.09, 0.10, 0.09
0.1–0.2	60	69.5, 0.11, 5.46, 3.55, 2.21	62.2, 0.01, 0.06, 0.06, 0.00
0.2–0.3	60	72.83, 0.08, 8.11, 2.91, 3.50	62.2, 0.01, 0.13, 0.14, 0.14
0.3–0.4	60	76.47, 0.10, 11.08, 3.90, 4.15	62.2, 0.10, 0.24, 0.24, 0.23
0.4–0.5	60	81.25, 0.06, 14.92, 4.73, 4.92	62.2, 0.10, 0.11, 0.09, 0.11

Table 4 System parameters

Item description	Values for simulation
source voltage	230 V, 50 Hz
linear load	Z = 200 +j 62.8Ω
other loads	rectifier
	(R L): 200+ j62.8Ω
800 VA	$V_{dc} = 320\,V, C_{dc} = 2\,mF$
UPQC	$L_1 = 2\,mH, L_2 = 0.4\,mH$
	$R_d = 5\Omega$
	$C = 36\,\mu F$
injection transformer	1 kVA

conventional UPQC deviates largely from the reference current. However, the source current follows the reference current in the proposed UPQC using a differential inverter. Even harmonics are very less in both topologies. Odd harmonic components are higher in conventional topology but, these are negligible in differential topology. Therefore, it can be concluded that the above-mentioned objectives are met and the proposed UPQC has an edge over the conventional UPQC.

7.3 Advantages and limitations of proposed UPQC

The current and voltage injection filtering inductance have supply voltage at one end and pole voltage of H bridge inverter at the other end. In conventional UPQC, the pole voltages continuously switch between $+V_{dc}/2$ and $-V_{dc}/2$ in a PWM manner. However, the pole voltage in the case of the differential inverter is a sinusoidal wave with a very small amount of ripple superimposed. The magnitude of this ripple can be reduced with an increase in switching frequency. With the advent of wide bandgap switching devices, one can go up to switching frequencies of MHz range. This may practically result in almost sinusoidal voltage at the pole voltage. In this case, this filtering inductance is not at all necessary in the circuit. Very low values of leakage inductance in the injection transformers will be capable of filtering action. In addition to the above, the advantages and limitations of proposed UPQC are summarised below.

i. A near sinusoidal waveform is obtained with only four switches per phase when compared with numerous switches required in multilevel inverters.
ii. The buck operation of individual buck circuits in the differential inverter is not passing through the zero cross over the region. Hence, the cross over distortion associated with similar buck inverter-based topologies is absent here.
iii. In total, 100% ripple cancellation is possible by proper synchronisation of triggering of both legs of the inverter.
iv. Active power decoupling facility can be implemented in the DC side without any additional switches or devices. Due to this, there will not be any second-order AC current and voltage in the dc side. So the life of BESS/battery is increased.
v. The requirement of large electrolytic capacitance in the DC side of the inverter is not necessary. Hence the failure rate of the inverter is reduced.
vi. The leakage current through the stray capacitance between the PV array and the ground is harmful. The CM connection of the differential inverter combined with a connection of resistance between neutral and ground can prevent this. This can be applied to all solar generation systems for residential application.
vii. Microinverters for grid-connected PV power conversion system often require voltage boost due to low DC voltage of the PV panels. The boost differential inverter connection ensures the required boost in voltage.
vii i. This can be extended to three-phase systems, as shown in Fig. 6. For the three-phase four-wire system we need to provide a star-delta transformer in front of the load and the neutral of the load need to be connected to the neutral point of the star side of the transformer. This connection will ensure the flow of unbalance current in the delta side of the transformer.
ix. The design is economical considering low DC link voltage, low capacity for BESS, the low voltage level for PV system and low rating of inverter switches. The DC link voltage of a conventional three-phase UPQC is more than twice the pole voltage. It is around 650 V or more to get a 400 V line to line voltage in the AC side. So the proposed topology using H-bridge will be economical in three-phase systems also.
x. We have to limit the load in the line to the thermal limit of the conductor. For the proposed AAC 7/3.1 conductor in the distribution line, the thermal limit is 160 A. In single phase, 230 V system, 1 kVA is 4.35 A. Therefore the capacity may be limited to 160/4.35, that equals 37 kVA for a single circuit. For three-phase system also the thermal limit is applicable, but the capacity can be three times more compared to single-phase systems. This limitation can be overcome if more circuits are added or by changing the conductor size with appropriate design for the overhead structure.

7.4 Hardware results

A prototype model of the UPQC of 800 VA capacity, using a differential inverter, is developed in the research laboratory with D-SPACE controller. The system parameters, as shown in Table 4, are used for the prototype implementation. The main objective is to maintain a constant voltage of 200 V to the sensitive load of 800 VA. Two inverter stack available in the research laboratory is connected as H-bridge for D-STATCOM and DVR. Each leg is controlled in DMs. Gating pulses are obtained from PWM generator with MATLAB and D-Space controller.

The injection transformer of 1 kVA rating and inductors 8 (Nos) are designed by us and made locally. Two current transformers (20/1 A) were purchased locally from a reputed manufacturer. Its secondary inputs were given to the ADC of D- Space Controller for current measurement. Filter capacitors were also purchased locally. Two numbers (230/1 V) transformers for taking secondary voltage to the ADC of D-Space Controller were designed by us and made locally. One of the secondary voltages of the transformer was given to ADC as the input of the PLL used for grid synchronisation. The second voltage transformer was used for measuring load-voltage.

The photograph of the hardware set up is shown in Fig. 19

The waveform showing the experimental results of the prototype model are shown in Figs. 20–25. Fig. 20 shows the reference load voltage of 200 V obtained using an auto transformer in the single-phase supply. Fig. 21 shows the waveform of source voltage and source current. The power factor is unity. Fig. 22 shows the D-STATCOM voltage and current before compensation. The current waveform is not sinusoidal due to non-linear loads. The current is slightly lagging due to the Inductive loading. Fig. 23 shows the waveform of the non-linear load alone. Fig. 24 shows the load voltage waveform of sag mitigation by the DVR. A sag of 20 V is initiated after a delay time using a delay timer and insertion of pre-determined resistance load in the load circuit. The DVR injects 20 V to the system and the voltage is maintained at 200 V. Fig. 25 shows the load voltage waveform of swell mitigation by the

Fig. 19 *Photograph of the hardware setup control of prototype model of UPQC at Resesrch Laboratory, GEC, Thrissur*

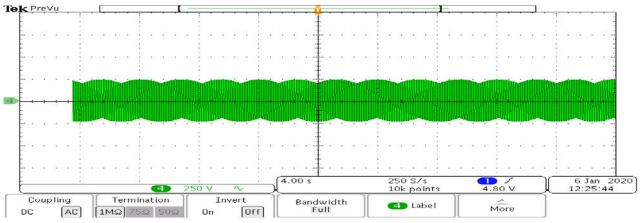

Fig. 20 *Waveform showing reference load voltage*

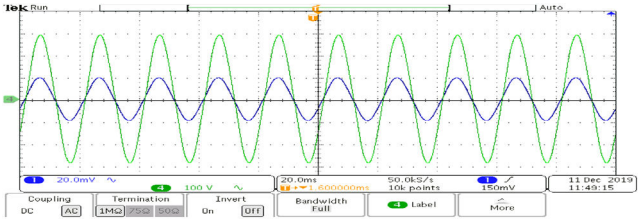

Fig. 21 *Waveform of source voltage and current after compensation*

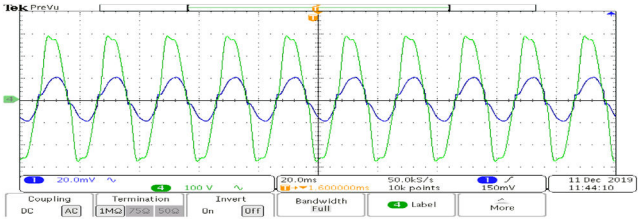

Fig. 22 *Waveform of D-statcom voltage and current before compensation*

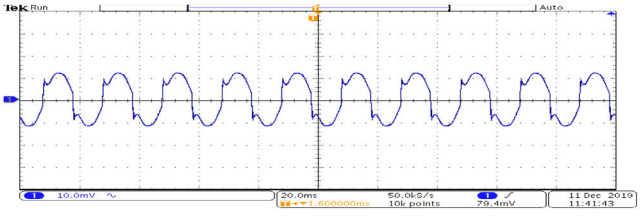

Fig. 23 *Waveform of current of non-linear load in ampere*

DVR. A swell of 20 V is initiated after a delay time using a delay timer and then there is removal of pre-determined resistance load in the load circuit. The DVR absorbs 20 V from the system, and the voltage is maintained at 200 V.

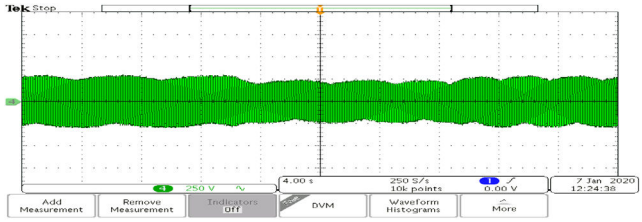

Fig. 24 *Waveform of load votage, first portion normal 200 V, second portion sag (180 V) and third portion DVR injection (200 V)*

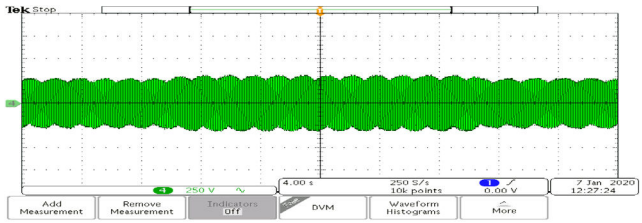

Fig. 25 *Waveform of load voltage first portion normal 200 V, second portion swell (220 V) and third portion DVR absorption (200V)*

8 Conclusion

The study simulates a 20 kVA, single-phase UPQC (using a PV-integrated distribution system for design) with a reduced DC link voltage of 360 V in MATLAB R2016a using ode23tb solver. The total load was 22 kVA in the system and the voltage is maintained at 226 V. To reduce THD, reactive load compensation of 10 kVAR and taking away the unwanted harmonics from the source were found to be sufficient. The source draws only active power, and the simulation results validated the input power factor as unity. The development of a prototype model of the UPQC of 800 VA capacity took place in our laboratory, by incorporating a 10 kW PV power into the grid and using a D-SPACE controller. The model achieved a load voltage of 200 V irrespective of sag and swell, with an economic model. This new design would find application in PV-integrated distribution systems and PV generating companies which need to integrate the PV generation to the utility grid for maintaining PQ standards. We have to limit the load in the line to the thermal limit of the conductor, therefore a higher capacity UPQC will be a limitation. We are planning to design and develop a three-phase, four-wire UPQC of 100 kVA rating, which is optimal for a healthcare facility/hospital.

9 References

[1] Donadel, C.B., Fardin, J.F., Encarnação, L.F.: 'Optimal placement of distributed generation units in a distribution system with uncertain topologies using monte carlo simulation', *Int. J. Emerging Electr. Power Syst.*, 2015, **16**, (5), pp. 431–441

[2] Donadel, C.B., Fardin, J.F., Encarnacao, L.F.: 'The influence of distributed generation units penetration in the technical planning process of electrical distribution networks', *IEEE Latin America Trans.*, 2017, **15**, (11), pp. 2144–2151

[3] I.P.W. Group, *, et al.*: 'Recommended practice for monitoring electric power quality'. Tech. Rep., Technical report, Draft 5, 1994

[4] Padiyar, K.: 'Facts controllers in power transmission and distribution', 2007

[5] Hingorani, N.G., Gyugyi, L., El-Hawary, M.: '*Understanding FACTS: concepts and technology of flexible AC transmission systems*', vol. **1** (Wiley Online Library, New York, NY, USA, 2000)

[6] Kundur, P., Balu, N.J., Lauby, M.G.: '*Power system stability and control*', vol. **7** (McGraw-hill, New York, 1994)

[7] Patel, A., Mathur, H.D., Bhanot, S.: 'A new srf-based power angle control method for upqc-dg to integrate solar pv into grid', *Int. Trans. Electr. Energy Syst.*, 2019, **29**, (1), p. e2667

[8] Chaudhary, P., Rizwan, M.: 'Voltage regulation mitigation techniques in distribution system with high pv penetration: a review', *Renew. Sustain. Energy Rev.*, 2018, **82**, pp. 3279–3287

[9] Luo, L., Gu, W., Zhang, X.-P., *et al.*: 'Optimal siting and sizing of distributed generation in distribution systems with pv solar farm utilized as statcom (pv-statcom)', *Appl. Energy*, 2018, **210**, pp. 1092–1100

[10] Sakar, S., Balci, M.E., Aleem, S.H.A., *et al.*: 'Integration of large-scale pv plants in non-sinusoidal environments: considerations on hosting capacity and harmonic distortion limits', *Renew. Sustain. Energy Rev.*, 2018, **82**, pp. 176–186

[11] Nieto, A., Vita, V., Maris, T.I.: 'Power quality improvement in power grids with the integration of energy storage systems', *Int. J. Eng. Res. Technol.*, 2016, **5**, (7), pp. 438–443
[12] Fujita, H., Akagi, H.: 'The unified power quality conditioner: the integration of series-and shunt-active filters', *IEEE Trans. Power Electron.*, 1998, **13**, (2), pp. 315–322
[13] Aredes, M., Heumann, K., Watanabe, E.H.: 'An universal active power line conditioner', *IEEE Trans. Power Deliv.*, 1998, **13**, (2), pp. 545–551
[14] Tolbert, L.M., Peng, F.Z., Habetler, T.G.: 'A multilevel converter-based universal power conditioner', *IEEE Trans. Ind. Appl.*, 2000, **36**, (2), pp. 596–603
[15] Ghosh, A., Ledwich, G.: 'A unified power quality conditioner (upqc) for simultaneous voltage and current compensation', *Electr. Power Syst. Res.*, 2001, **59**, (1), pp. 55–63
[16] Haghighat, H., Seifi, H., Yazdian, A.: 'An instantaneous power theory based control scheme for unified power flow controller in transient and steady state conditions', *Electr. Power Syst. Res.*, 2003, **64**, (3), pp. 175–180
[17] Han, B., Bae, B., Baek, S.*, et al.*: 'New configuration of upqc for medium-voltage application', *IEEE Trans. Power Deliv.*, 2006, **21**, (3), pp. 1438–1444
[18] Kolhatkar, Y.Y., Das, S.P.: 'Experimental investigation of a single-phase upqc with minimum va loading', *IEEE Trans. Power Deliv.*, 2006, **22**, (1), pp. 373–380
[19] Central Electricity Regulatory Commission Commission, *, et al.*: 'Indian electricity grid code', Effective from 1st April, 2006
[20] Pawar, S.S., Deshpande, A., Murali, M.: 'Modelling and simulation of dstatcom for power quality improvement in distribution system using matlab simulink tool'. 2015 Int. Conf. on Energy Systems and Applications, Pune, India, 2015, pp. 224–227
[21] Saradva, P.M., Kadivar, K.T., Pandya, M.H.*, et al.*: 'Reactive and real power compensation in distribution line using d-statcom with energy storage'. 2016 Int. Conf. on Computation of Power, Energy Information and Commuincation (ICCPEIC), Chennai, India, 2016, pp. 726–732
[22] Singh, B., Jayaprakash, P., Kothari, D.P.*, et al.*: 'Comprehensive study of dstatcom configurations', *IEEE Trans. Ind. Inf.*, 2014, **10**, (2), pp. 854–870
[23] Bina, M.T., Eskandari, M., Panahlou, M.: 'Design and installation of a± 250 kvar d-statcom for a distribution substation', *Electr. Power Syst. Res.*, 2005, **73**, (3), pp. 383–391
[24] Singh, B., Solanki, J.: 'A comparative study of control algorithms for dstatcom for load compensation'. IEEE Int. Conf. on Industrial Technology, 2006. ICIT 2006, Mumbai, India, 2006, pp. 1492–1497
[25] Yao, W., Wang, X., Zhang, X.*, et al.*: 'A unified active damping control for single-phase differential mode buck inverter with lcl-filter'. 2015 IEEE Sixth Int. Symp. on Power Electronics for Distributed Generation Systems (PEDG), Aachen, Germany, 2015, pp. 1–8
[26] Kumar, C., Mishra, M.K.: 'A modified dstatcom topology with reduced vsi rating, dc link voltage, and filter size'. 2013 Int. Conf. on Clean Electrical Power (ICCEP), Alghero, Italy, 2013, pp. 325–331